Mössbauer effect study of the decagonal quasicrystal $Al_{70}Co_{15}Ni_{15}$

# Mössbauer effect study of the decagonal quasicrystal Al$_{70}$Co$_{15}$Ni$_{15}$

**Zbigniew M Stadnik**[1,3] **and Guowei Zhang**[2]

[1] Department of Physics, University of Ottawa, Ottawa, ON, K1N 6N5, Canada
[2] Department of Radiation Oncology, University of Maryland, Baltimore, MD 21201, USA

**Abstract**

We present a systematic $^{57}$Fe Mössbauer effect study in the temperature range between 5.3 and 298.2 K and in an external magnetic field of 9.0 T of a high-quality stable decagonal quasicrystal Al$_{70}$Co$_{15}$Ni$_{14.9}$Fe$_{0.1}$. The iron atoms are shown to be located in two distinct classes of sites. The values of the principal component of the electric field gradient tensor and the asymmetry parameter at these sites are, respectively, $-1.901(61) \times 10^{21}$ V m$^{-2}$, 0.96(12) and $-3.927(52) \times 10^{21}$ V m$^{-2}$, 0.27(9). The average quadrupole splitting decreases with temperature as $T^{3/2}$. The vibrations of the Fe atoms are well described by a Debye model, with the Debye temperature of 546(9) K.

## 1. Introduction

Quasicrystals (QCs) are intermetallic alloys that possess a new type of long-range translational order, *quasiperiodicity*, and a noncrystallographic orientational order associated with the classically forbidden fivefold (icosahedral), eightfold (octagonal), tenfold (decagonal), and twelvefold (dodecagonal) symmetry axes [1]. A central problem in studies of QCs is determining their atomic structure, which is a prerequisite for understanding many unusual physical properties of these alloys. In spite of significant progress in recent years, the complete determination of the structure of QCs has not yet been accomplished [2].

Since Tsai *et al* [3] found a stable and highly ordered decagonal QC Al$_{70}$Co$_{15}$Ni$_{15}$, the Al–Co–Ni phases have been the most extensively studied among decagonal QCs. There are several quantitative x-ray diffraction (XRD) studies of the structure of the decagonal Al–Ni–Co system using the five-dimensional description of the structure of a decagonal QC [4]. The difficulty with the five-dimensional approach is that only an average structure can be determined, as disorder in a decagonal QC cannot be treated properly. The relatively small number of Bragg reflections available [2] leads to some spurious atoms with unphysical inter-atomic separations in structural models. In addition, a problem of XRD analysis is that it is not

---

[3] Author to whom any correspondence should be addressed.

possible to distinguish between the different transition metal (TM) atoms in the ternary Al–Ni–Co QC. It appears that the XRD investigations alone might not be able to solve for the structure of the decagonal Al–Ni–Co QC. A large number of electron microscopy structural studies have been carried out on the decagonal Al–Ni–Co QC [5]. These studies reveal the local projected structure in the decagonal Al–Ni–Co QC that consists of 2 nm diameter cluster columns. Similarly to the XRD investigation case, the TM atoms are not distinguished. Recently, total-energy calculations, based on pair potentials derived from first-principles electronic structure considerations and using a minimum of experimental XRD information, have been employed to predict the structure of the decagonal Al–Ni–Co QC [6]. The structural model determined, in which TM atoms are clearly distinguished, is generally consistent with XRD and $Z$-contrast electron microscopy data [6]. A nonlinear least-squares analysis combining XRD data and results from total-energy calculations [7] seems to be a promising new approach for determining the structure of the decagonal Al–Ni–Co QC.

Complementary to the above-discussed methods of structure determination are the approaches using local probes, such as extended x-ray absorption fine structure (EXAFS), nuclear quadrupole resonance (NQR), and Mössbauer spectroscopy (MS), which are element selective and sensitive to the local atomic structure. It has been recently demonstrated [8] how the combination of the complete set of MS data and the calculations of the electric field gradients (EFGs) for several XRD-based structural models of the icosahedral Al–Cu–Fe QC led to a solution for the structure of this QC. There has been only one quantitative EXAFS study of the local structure of the decagonal Al–Ni–Co QC [9].

The main objective of the present study is to provide a complete set of the EFG parameters at the TM sites in the decagonal Al–Ni–Co QC.

## 2. Experimental procedure

An ingot of nominal composition $Al_{70}Co_{15}Ni_{14.9}Fe_{0.1}$ was prepared by the melting in an argon atmosphere of high-purity constituent elements; the Fe metal used was enriched to 95.9% in the $^{57}Fe$ isotope. The ingot was annealed in vacuum at 1070 K for 48 h.

XRD data were collected at 298 K in Bragg–Brentano geometry using a PANanalytical X'Pert diffractometer equipped with a PW3020 vertical goniometer with a 173 mm radius and with a long fine focus Cu target x-ray tube operated at 45 kV and 40 mA. The diffractometer was equipped with a variable divergence slit which kept the illuminated length of the sample constant at 12.5 mm. XRD data were collected by step scanning in the $2\theta$ range 5°–132° with a step size of 0.02° and a count time of 9 s/step. A fine sample powder was mixed with methanol and allowed to dry on a low-background sample holder; the result was a thin flat sample. A sample spinner was used to minimize possible preferred sample orientation. Corrections for instrumental aberration and specimen displacement were made on $2\theta$ angles from the scan of the specimen containing the Si internal standard (National Institute of Standards and Technology reference material 640c). Cu K$\alpha$ radiation was employed and the K$\beta$ line was eliminated by using a Kevex PSi2 Peltier cooled Si detector.

$^{57}Fe$ MS measurements were performed in the temperature range 5.3–298.2 K using a standard Mössbauer spectrometer operating in a sine mode and a source of $^{57}Co(Rh)$ at room temperature. Mössbauer spectra in an external magnetic field of 9.0 T parallel to the $\gamma$-ray propagation direction were measured with the $^{57}Co(Rh)$ source held at the same temperature as the sample. The spectrometer was calibrated with a 6.35 $\mu$m $\alpha$-Fe foil (the surface density was $107 \times 10^{-3}$ mg $^{57}Fe$ cm$^{-2}$) [10], and the spectra were folded. The full linewidth at half-maximum of the inner pair of the $\alpha$-Fe Zeeman pattern was 0.2244(40) mm s$^{-1}$ and this value can be regarded as the resolution of the Mössbauer spectrometer. The Mössbauer absorber
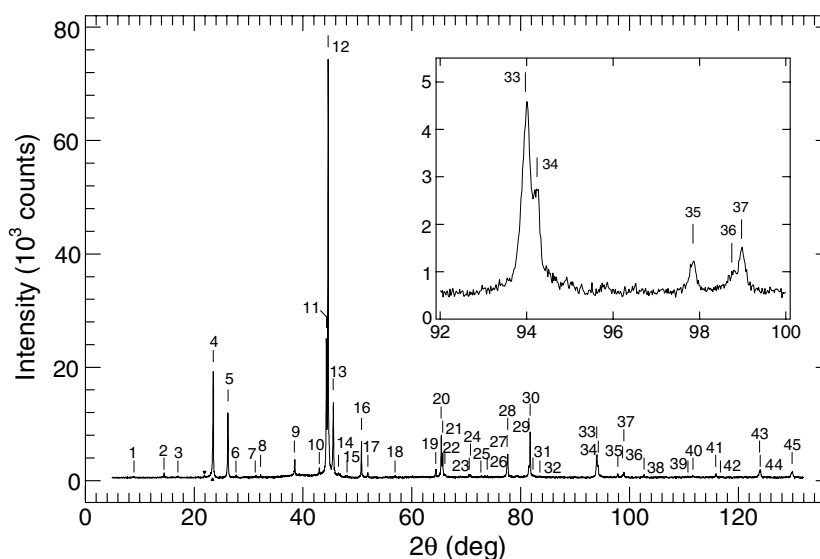
**Figure 1.** The XRD spectrum of an $Al_{70}Co_{15}Ni_{14.9}Fe_{0.1}$ alloy at 298 K corrected for the background and the Cu $K\alpha_2$ lines. The vertical lines labelled with integers above all detected decagonal Bragg peaks correspond to the positions calculated for the Cu $K\alpha_1$ radiation, as explained in the text. The position, full width at half-maximum, and relative intensity of each detected decagonal peak are given in table 1 together with the corresponding index. The symbols ▼ and ▲ indicate the peak positions corresponding to an unidentified second phase. The inset shows a part of the spectrum with low-intensity lines.

was prepared by mixing the powdered alloy with powdered BN to ensure a uniform thickness of the absorber and the random orientation of sample particles. This mixture was then put into a plastic sample holder. The surface density of the Mössbauer absorber was $36 \times 10^{-3}$ mg $^{57}$Fe cm$^{-2}$. This corresponds to the effective thickness parameter [11] at 5.3 K of 0.93 (using the value of the absorber Lamb–Mössbauer factor at 5.3 K of 0.94 found from the Debye temperature of 546 K determined below). As the resulting Mössbauer spectra are due to a multiple of the elementary quadrupole doublet, the effective thickness parameter spreads over them and therefore the absorbers can be regarded as being thin [11].

## 3. Results and discussion

### 3.1. Structural characterization

The XRD spectrum of the alloy studied measured in the $2\theta$ range 5°–132° (figure 1) shows the presence of 45 Bragg peaks due to the decagonal structure and two very weak peaks due to an unidentified second phase. The positions of all detected Bragg peaks due to the decagonal structure corresponding to Cu $K\alpha_1$ radiation (the value of its wavelength $\lambda$ currently accepted by the National Institute for Standards and Technology is 1.540 5981 Å [12]) in terms of the angle $2\theta_1$ and the corresponding wavenumber $Q_{exp} = 4\pi \sin\theta_1/\lambda$, as well as their relative intensities and full widths at half-maximum $\Gamma_Q$, were determined from the profile fitting using the procedure described in [13], and are given in table 1. Bragg peaks have been indexed following the scheme of Yamamoto and Ishihara [14]. Table 1 contains also the theoretical positions $Q_{cal}$, which were calculated by taking the positions of peak numbers 12 and 43 as reference positions, as well as the indices of all Bragg peaks. This analysis yields a quasilattice

**Table 1.** Positions in terms of $2\theta_1$ (in deg) corresponding to Cu K$\alpha_1$ radiation and $Q_{exp}$ (in Å$^{-1}$), full width at half-maximum $\Gamma_Q$ (in Å$^{-1}$), and relative intensity INT normalized to 100.0 of all detected decagonal Bragg peaks, which are labelled with consecutive integers in column 1, as obtained from the fit [13]. The integers correspond to the vertical lines in figure 1. $Q_{cal}$ (in Å$^{-1}$) is the $Q$ value calculated by taking the positions of peak numbers 12 and 43 as reference positions. Index refers to indices of the decagonal Bragg peaks based on the indexing scheme of Yamamoto and Ishihara [14].

| Label | $2\theta_1$ | $Q_{exp}$ | $Q_{cal}$ | $\Gamma_Q$ | INT | Index |
|---|---|---|---|---|---|---|
| 1 | 8.937 | 0.636 | 0.634 | 0.017 | 0.4 | 00110 |
| 2 | 14.470 | 1.027 | 1.026 | 0.013 | 1.4 | 01210 |
| 3 | 17.014 | 1.207 | 1.206 | 0.012 | 0.5 | 01220 |
| 4 | 23.489 | 1.660 | 1.660 | 0.010 | 27.5 | 02320 |
| 5 | 26.200 | 1.849 | 1.849 | 0.010 | 14.2 | 01211 |
| 6 | 27.683 | 1.951 | 1.952 | 0.012 | 0.7 | 13420 |
| 7 | 31.383 | 2.206 | 2.205 | 0.012 | 0.4 | 02430 |
| 8 | 32.206 | 2.262 | 2.263 | 0.010 | 0.6 | 02321 |
| 9 | 38.427 | 2.684 | 2.686 | 0.013 | 5.4 | 01511 |
| 10 | 42.999 | 2.989 | 2.988 | 0.014 | 2.2 | 14521 |
| 11 | 44.301 | 3.075 | 3.076 | 0.014 | 42.4 | 00002 |
| 12 | 44.605 | 3.095 | 3.095 | 0.009 | 100.0 | 03531 |
| 13 | 45.559 | 3.158 | 3.158 | 0.012 | 25.4 | 15630 |
| 14 | 46.528 | 3.222 | 3.221 | 0.009 | 0.7 | 03640 |
| 15 | 48.087 | 3.323 | 3.322 | 0.007 | 0.3 | 14631 |
| 16 | 50.729 | 3.494 | 3.495 | 0.009 | 8.7 | 00650 |
| 17 | 51.899 | 3.569 | 3.569 | 0.011 | 1.5 | 34432 |
| 18 | 56.906 | 3.886 | 3.887 | 0.012 | 0.6 | 16710 |
| 19 | 64.422 | 4.348 | 4.348 | 0.012 | 3.3 | 01552 |
| 20 | 65.414 | 4.407 | 4.407 | 0.010 | 11.7 | 25951 |
| 21 | 65.670 | 4.423 | 4.422 | 0.010 | 7.2 | 16841 |
| 22 | 66.048 | 4.445 | 4.446 | 0.024 | 1.3 | 03851 |
| 23 | 70.546 | 4.710 | 4.711 | 0.009 | 0.8 | 15742 |
| 24 | 70.787 | 4.724 | 4.725 | 0.009 | 0.8 | 06870 |
| 25 | 72.679 | 4.834 | 4.834 | 0.015 | 0.5 | 16951 |
| 26 | 73.877 | 4.902 | 4.901 | 0.011 | 0.3 | 38 10 70 |
| 27 | 77.505 | 5.106 | 5.105 | 0.015 | 3.5 | 01433 |
| 28 | 77.623 | 5.112 | 5.113 | 0.009 | 6.5 | 01513 |
| 29 | 81.506 | 5.325 | 5.325 | 0.013 | 4.0 | 05852 |
| 30 | 81.739 | 5.337 | 5.337 | 0.008 | 10.0 | 02 10 61 |
| 31 | 82.258 | 5.365 | 5.367 | 0.025 | 1.6 | 01862 |
| 32 | 83.558 | 5.435 | 5.434 | 0.011 | 0.4 | 00 10 70 |
| 33 | 93.980 | 5.965 | 5.964 | 0.012 | 10.7 | 28 10 52 |
| 34 | 94.246 | 5.977 | 5.977 | 0.009 | 4.6 | 28 10 62 |
| 35 | 97.841 | 6.149 | 6.149 | 0.009 | 1.9 | 26 14 30 |
| 36 | 98.747 | 6.191 | 6.191 | 0.017 | 1.6 | 06 10 62 |
| 37 | 98.981 | 6.202 | 6.201 | 0.008 | 1.5 | 05 12 70 |
| 38 | 102.669 | 6.369 | 6.370 | 0.009 | 1.2 | 03943 |
| 39 | 110.724 | 6.711 | 6.711 | 0.019 | 0.8 | 3 10 13 91 |
| 40 | 111.708 | 6.751 | 6.750 | 0.009 | 0.7 | 29 13 81 |
| 41 | 115.872 | 6.913 | 6.911 | 0.006 | 1.1 | 05 11 92 |
| 42 | 116.739 | 6.945 | 6.945 | 0.005 | 0.2 | 03644 |
| 43 | 123.908 | 7.199 | 7.199 | 0.014 | 5.0 | 08 13 81 |
| 44 | 124.064 | 7.204 | 7.204 | 0.005 | 0.9 | 3 10 15 60 |
| 45 | 129.886 | 7.389 | 7.389 | 0.011 | 5.4 | 17724 |
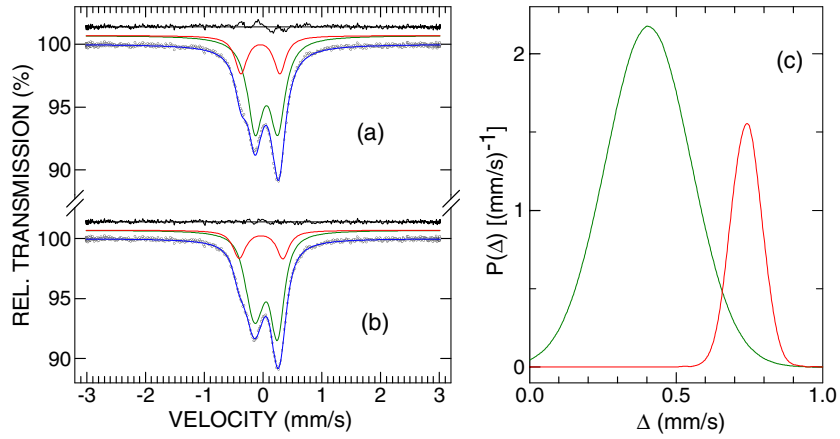
**Figure 2.** The $^{57}$Fe Mössbauer spectrum of the decagonal $Al_{70}Co_{15}Ni_{14.9}Fe_{0.1}$ alloy at 5.3 K fitted (solid curve) (a) with two symmetric quadrupole doublets and (b) with two $P(\Delta)$ components shown in (c). The zero of the velocity scale in (a) and (b) is relative to the $^{57}$Co(Rh) source at 5.3 K. The residuals are shown above each spectrum.

parameter $a = 7.170$ Å perpendicular to the tenfold axis and a quasilattice stacking periodicity $c = 4.085$ Å along the tenfold axis.

There is an excellent agreement between the observed $Q_{exp}$ and the theoretical $Q_{cal}$ positions of the decagonal Bragg peaks (figure 1 and table 1). The widths $\Gamma_Q$ of most decagonal peaks are found to be limited by the instrumental resolution, which is indicative of a high degree of structural order. The values of the lattice parameters $a$ and $c$ are consistent with the previously published values for a decagonal QC of similar composition [15].

### 3.2. Mössbauer spectroscopy

The low-temperature Mössbauer spectrum of the decagonal $Al_{70}Co_{15}Ni_{14.9}Fe_{0.1}$ QC (figure 2(a)), in contrast to Mössbauer spectra of icosahedral QCs which are in the form of a somewhat broadened single quadrupole doublets [16], exhibits a clear structure. It can be fitted unequivocally with two symmetric quadrupole doublets (figure 2(a)). Each doublet is characterized by a full linewidth at half-maximum $\Gamma$, a relative area $A$, a centre shift $\delta$ (relative to $\alpha$-Fe at 298 K), and a quadrupole splitting [11]

$$\Delta = \tfrac{1}{2} e Q \, |V_{zz}| \, (1 + \tfrac{1}{3}\eta^2)^{1/2}, \tag{1}$$

where $e$ is the proton charge and $Q$ is the electric quadrupole moment of the nucleus. The asymmetry parameter $\eta = (V_{xx} - V_{yy})/V_{zz}$ $(0 \leqslant \eta \leqslant 1)$, where $V_{xx}$, $V_{yy}$, and $V_{zz}$ are the eigenvalues of the electric field gradient (EFG) tensor in order of increasing magnitude [11]. The values of $\Gamma$, $A$, $\delta$, $\Delta$ determined from the fit ($\chi^2 = 1.74$) for each quadrupole doublet are, respectively, 0.3117(45) mm s$^{-1}$, 74.8(1.4)%, 0.2984(15) mm s$^{-1}$, 0.3830(37) mm s$^{-1}$ and 0.2478(89) mm s$^{-1}$, 25.2(1.4)%, 0.1956(35) mm s$^{-1}$, 0.6593(63) mm s$^{-1}$. The fact that the Mössbauer spectrum of the decagonal $Al_{70}Co_{15}Ni_{14.9}Fe_{0.1}$ QC is unquestionably composed of two quadrupole doublets (figure 1(a)) proves the existence of two distinct iron sites in this QC.

The values of $\Gamma$ corresponding to the two component quadrupole doublets are larger than the value of 0.2244(40) mm s$^{-1}$ obtained from the velocity calibration with a 6.35 $\mu$m $\alpha$-Fe foil. This line broadening indicates the presence of the distribution $P(\Delta)$ of the quadrupole splittings. The distribution $P(\Delta)$ is the consequence of
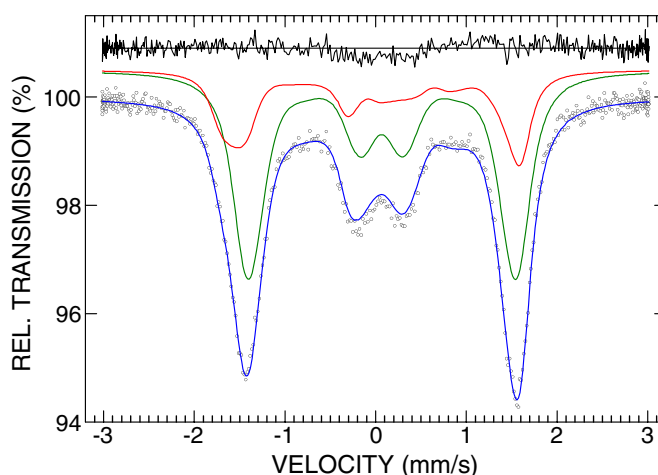
**Figure 3.** The $^{57}$Fe Mössbauer spectrum of the decagonal $Al_{70}Co_{15}Ni_{14.9}Fe_{0.1}$ alloy at 5.4 K in an external magnetic field of 9.0 T fitted (solid line) with two components. The zero velocity scale is relative to the $^{57}$Co(Rh) source at 5.4 K. The residuals are shown above the spectrum.

the distributions of the EFG and of the asymmetry parameter. The low-temperature Mössbauer spectrum of the decagonal $Al_{70}Co_{15}Ni_{14.9}Fe_{0.1}$ QC (figure 2(b)) was fitted with the constrained version [17] of the Hesse–Rübartsch method [18]. A linear relation between $\delta$ and $\Delta$ for the elementary Lorentzian doublets of the full linewidth at half-maximum $\Gamma$ was assumed. A small distribution of $\delta$, independent of EFG, was assumed and characterized by the standard deviation parameter $\sigma_\delta$. A satisfactory fit ($\chi^2 = 1.13$; figure 2(b)) was obtained for the distributions $P(\Delta)$ shown in figure 2(c). The parameters $A$, $\bar{\delta}$, $\sigma_{\bar{\delta}}$, the average quadrupole splitting $\bar{\Delta}$, and its standard deviation $\sigma_{\bar{\Delta}}$ obtained from the fit corresponding to two $P(\Delta)$ components are, respectively, 79.1(3.5)%, 0.2895(142) mm s$^{-1}$, 0.0215(20) mm s$^{-1}$, 0.3880(11) mm s$^{-1}$, 0.1315(12) mm s$^{-1}$ and 20.9(3.4)%, 0.2070(310) mm s$^{-1}$, 0.0035(3) mm s$^{-1}$, 0.7398(105) mm s$^{-1}$, 0.0531(103) mm s$^{-1}$, and the value of $\Gamma$ was 0.2423(132) mm s$^{-1}$. A successful fit of the Mössbauer spectrum of the decagonal $Al_{70}Co_{15}Ni_{14.9}Fe_{0.1}$ QC with two $P(\Delta)$ components provides evidence for the existence of two distinct classes of iron sites in this QC.

The fits of the zero-field Mössbauer spectrum in figure 2 give information on the magnitude of $\Delta$, but not on the sign of the main component of the EFG, $V_{zz}$, or the value of $\eta$. Complete information on the sign of $V_{zz}$ and the value of $\eta$ can be obtained from the Mössbauer spectra measured in external magnetic fields such that the magnetic dipole interaction becomes of similar magnitude to the electric quadrupole interaction. To determine the sign of $V_{zz}$ and the value of $\eta$ for the QC studied, a Mössbauer spectrum was measured in an external magnetic field of 9.0 T (figure 3). The Mössbauer spectra exhibiting mixed hyperfine magnetic dipole and electric quadrupole interactions must be treated using the exact Hamiltonian [11]. If texture effects are negligible one can assume, similarly to the case for powder samples, that the principal axes of the EFG tensor are randomly oriented with respect to the external magnetic field. The algorithm for calculating the spectra in such a case was given by Blaes *et al* [19] and was used to fit the spectrum in figure 3. As there are two classes of iron sites (figure 2), it is clear that there are four possible combinations of signs for $q = \frac{1}{2}eQV_{zz}$: $(+, +)$, $(+, -)$, $(-, -)$, and $(-, +)$. The Mössbauer spectrum in figure 3 was fitted with two components corresponding to these four combinations of $q$ signs; the value of $\Gamma$ for two component subspectra was taken
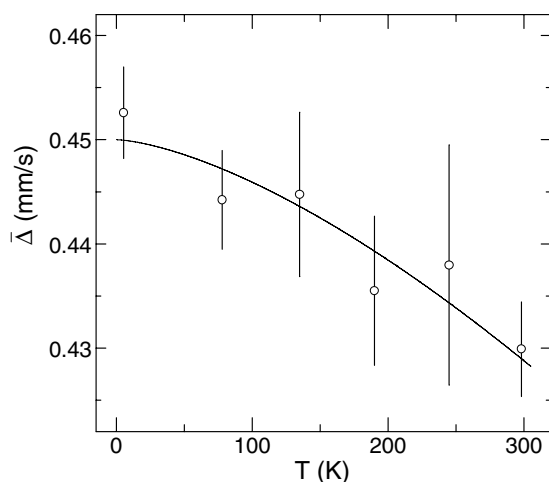
**Figure 4.** The temperature dependence of the average quadrupole splitting of the decagonal $Al_{70}Co_{15}Ni_{14.9}Fe_{0.1}$ alloy. The solid curve is the fit to equation (2), as explained in the text.

from the zero-field fit (figure 2(a)) and was fixed in the fit, and the hyperfine magnetic field $B_{hf}$ was a fitted parameter. The best fit ($\chi^2 = 1.58$; figure 3) was obtained for $B_{hf} = 8.9(1)$ T, which is very close to the applied magnetic field of 9.0 T, and for the following values of $A$, $\delta$, $q$, $\eta$ corresponding, respectively, to two iron sites: 69.0(2.5)%, 0.3091(21) mm s$^{-1}$, $-0.3164(102)$ mm s$^{-1}$, 0.96(12) and 31.0(2.3)%, 0.2232(58) mm s$^{-1}$, $-0.6534(86)$ mm s$^{-1}$, 0.27(9). Thus, $V_{zz}$ is negative at two iron sites and has the values of $-1.901(61) \times 10^{21}$ and $-3.927(52) \times 10^{21}$ V m$^{-2}$. In converting from the measured $q$ to $V_{zz}$ we have used the value $Q = 16$ fm$^2$, which is based on a systematic comparison of experimentally determined quadrupole splittings and calculated EFGs [20] and which has been confirmed by a nuclear shell-model calculation [21].

The analysis presented above enabled us to determine precisely the values of the EFG at the two classes of iron sites in the decagonal $Al_{70}Co_{15}Ni_{14.9}Fe_{0.1}$ QC. What is now required is *ab initio* calculation of the EFGs for the Al–Co–Ni QC for several available structural models [4–7] of this QC. Comparing these calculated EFGs with the experimentally determined EFG here, similarly to what has been done for the icosahedral Al–Cu–Fe QC [8], could lead to the solution of the structure of the decagonal Al–Ni–Co QC.

$^{57}$Fe Mössbauer spectra of the decagonal $Al_{70}Co_{15}Ni_{14.9}Fe_{0.1}$ QC were measured at other temperatures. They all exhibit the same two-component structure as was observed in the spectrum at 5.3 K (figure 2(a)). As a general trend, the average value of the quadrupole splitting $\bar{\Delta}$ decreases with increasing temperature. The temperature dependence of $\bar{\Delta}$ could be fitted (figure 4) to the empirical equation

$$\bar{\Delta}(T) = \bar{\Delta}(0)(1 - BT^{3/2}), \tag{2}$$

where $\bar{\Delta}(0)$ is the value of $\bar{\Delta}$ at 0 K and $B$ is a constant. Such a $T^{3/2}$ temperature dependence has been observed for many metallic noncubic crystalline alloys [22], for some amorphous [23, 24] alloys, and recently for icosahedral QCs [24, 25] over temperature ranges from a few kelvins to the melting point. This seemingly universal $T^{3/2}$ dependence is not well understood. Its origin seems to be associated with a strong temperature dependence of mean square lattice displacements and, to a lesser extent, with the temperature dependence of the lattice expansion [26]. The values of $\bar{\Delta}(0)$, $B$ determined from the fit for decagonal
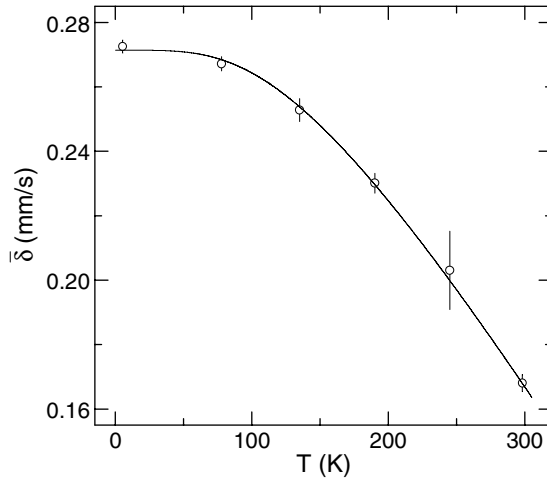
**Figure 5.** The temperature dependence of the average centre shift of the decagonal $Al_{70}Co_{15}Ni_{14.9}Fe_{0.1}$ alloy. The solid curve is the fit to equation (3), as explained in the text.

$Al_{70}Co_{15}Ni_{14.9}Fe_{0.1}$ QC are 0.4501(17) mm s$^{-1}$, $9.07(1.31) \times 10^{-6}$ K$^{-3/2}$. The value of $B$ is similar to that found for other metallic amorphous and icosahedral alloys [23–25].

The average centre shift at temperature $T$, $\bar{\delta}(T)$, determined from the fits of the spectra of the sample studied measured at different temperatures is given by

$$\bar{\delta}(T) = \delta_0 + \delta_{SOD}(T), \tag{3}$$

where $\delta_0$ is the intrinsic isomer shift and $\delta_{SOD}(T)$ is the second-order Doppler (SOD) shift which depends on lattice vibrations of the Fe atoms [11]. In terms of the Debye approximation of the lattice vibrations, $\delta_{SOD}(T)$ is expressed [11] in terms of the Debye temperature, $\Theta_D$, as

$$\delta_{SOD}(T) = -\frac{9}{2}\frac{k_B T}{Mc}\left(\frac{T}{\Theta_D}\right)^3 \int_0^{\Theta_D/T} \frac{x^3\,\mathrm{d}x}{\mathrm{e}^x - 1}, \tag{4}$$

where $M$ is the mass of the Mössbauer nucleus and $c$ is the speed of light. By fitting the experimental data $\bar{\delta}(T)$ (figure 5) to equation (3), the quantities $\delta_0$ and $\Theta_D$ were found to be, respectively, 0.2714(7) mm s$^{-1}$ and 546(9) K. The value of $\Theta_D$ found here differs significantly from the value of 123 K reported for the decagonal $Al_{73}Co_{17}Ni_{10}$ QC [27] and is comparable to the values of 589(12) K found for the decagonal $Al_{71}Co_{13}Ni_{16}$ QC [28] and of 596 K found for the decagonal $Al_{65}Co_{15}Cu_{20}$ QC [29]. The values of $\Theta_D$ for stable decagonal QCs [28, 29] are significantly larger than those for stable icosahedral QCs [25].

## 4. Conclusions

A systematic $^{57}$Fe Mössbauer effect study in the temperature range between 5.3 and 298.2 K and in an external magnetic field of 9.0 T on a high-quality stable decagonal quasicrystal $Al_{70}Co_{15}Ni_{14.9}Fe_{0.1}$ has been presented. The iron atoms are shown to be located in two distinct classes of sites. The values of the principal component of the electric field gradient tensor and the asymmetry parameter at these sites are determined to be, respectively, $-1.901(61) \times 10^{21}$ V m$^{-2}$, 0.96(12) and $-3.927(52) \times 10^{21}$ V m$^{-2}$, 0.27(9). The average quadrupole splitting is shown to decrease with temperature as $T^{3/2}$. The vibrations of the Fe

atoms are well described by a Debye model, with the Debye temperature of 546(9) K, which is considerably higher than the Debye temperatures previously reported for stable icosahedral quasicrystals.

## Acknowledgment

## References

[1] Stadnik Z M (ed) 1999 *Physical Properties of Quasicrystals* (Berlin: Springer)
[2] Steurer W 2004 *J. Non-Cryst. Solids* **334/335** 137
[3] Tsai A-P, Inoue A and Masumoto T 1989 *Mater. Trans. JIM* **30** 463
[4] Yamamoto A, Kato K, Shibuya T and Takeuchi S 1990 *Phys. Rev. Lett.* **65** 1603
    Steurer W, Haibach T, Zhang B, Kek S and Lück R 1993 *Acta Crystallogr.* B **49** 661
    Elcoro L and Perez-Mato J M 1995 *J. Physique* I **5** 729
    Takakura H, Yamamoto A and Tsai A P 2001 *Acta Crystallogr.* A **57** 576
    Cervellino A, Haibach T and Steurer W 2002 *Acta Crystallogr.* B **58** 8
[5] Saitoh K, Tsuda K, Tanaka M, Kaneko K and Tsai A P 1997 *Japan. J. Appl. Phys.* **36** L1400
    Saitoh K, Tsuda K and Tanaka M 1998 *J. Phys. Soc. Japan* **67** 2578
    Steinhardt P J, Jeong H-C, Saitoh K, Tanaka M, Abe E and Tsai A P 1998 *Nature* **396** 55
    Yan Y, Pennycook S J and Tsai A P 1998 *Phys. Rev. Lett.* **81** 5145
    Yan Y and Pennycook S J 1999 *Nature* **403** 266
    Steinhardt P J, Jeong H-C, Saitoh K, Tanaka M, Abe E and Tsai A P 1999 *Nature* **403** 267
    Abe E, Saitoh K, Takakura H, Tsai A P, Steinhardt P J and Jeong H-C 2000 *Phys. Rev. Lett.* **84** 4609
    Yan Y and Pennycook S J 2000 *Phys. Rev.* B **61** 14291
    Saitoh K, Tsuda K, Tanaka M and Tsai A P 2000 *Z. Kristallogr.* **215** 618
[6] Yan Y and Pennycook S J 2001 *Phys. Rev. Lett.* **86** 1542
    Mihalkovič M, Al-Lehyani I, Cockayne E, Henley C L, Moghadam N, Moriarty J A, Wang Y and Widom M 2002 *Phys. Rev.* B **65** 104205
[7] Mihalkovič M, Henley C L and Widom M 2004 *J. Non-Cryst. Solids* **334/335** 177
[8] Zijlstra E S, Kortus J, Krajčí M, Stadnik Z M and Bose S K 2004 *Phys. Rev.* B **69** 094206
[9] Zaharko O, Mengeghini C, Cervellino A and Fisher E 2001 *Eur. Phys. J.* B **19** 207
[10] Cali J P (ed) 1971 Certificate of Calibration, Iron Foil Mössbauer Standard, NBS Circular No 1541 (Washington, DC: US Government Printing Office)
[11] Greenwood N N and Gibb T C 1971 *Mössbauer Spectroscopy* (London: Chapman and Hall)
    Gütlich P, Link R and Trautwein A 1978 *Mössbauer Spectroscopy and Transition Metal Chemistry* (Berlin: Springer)
[12] Jenkins R and Schreiner W N 1989 *Powder Diffr.* **4** 74
[13] Schreiner W N and Jenkins R 1983 *Adv. X-ray Anal.* **26** 141
[14] Yamamoto A and Ishihara K N 1988 *Acta Crystallogr.* A **44** 707
[15] Kupsch A, Meyer D C, Gille P and Paufler P 2002 *J. Alloys Compounds* **342** 256
[16] Stadnik Z M 1996 *Mössbauer Spectroscopy Applied to Magnetism and Materials Science* vol 2, ed G J Long and F Grandjean (New York: Plenum) p 125
[17] Le Caër G and Dubois J M 1979 *J. Phys. E: Sci. Instrum.* **12** 1083
[18] Hesse J and Rübartsch A 1974 *J. Phys. E: Sci. Instrum.* **7** 526
[19] Blaes N, Fischer H and Gonser U 1985 *Nucl. Instrum. Methods Phys. Res.* B **9** 201
[20] Dufek P, Blaha P and Schwarz K 1995 *Phys. Rev. Lett.* **75** 3545
[21] Martínez-Pinedo G, Schwerdtfeger P, Caurier E, Langanke K, Nazarewicz W and Söhnel T 2001 *Phys. Rev. Lett.* **87** 062701
[22] Kaufmann E N and Vianden R J 1979 *Rev. Mod. Phys.* **51** 161 and references therein
[23] Deppe P and Rosenberg M 1983 *Hyperfine Interact.* **15/16** 735
    Kopcewicz M, Kopcewicz B and Gonser U 1987 *J. Magn. Magn. Mater.* **66** 79
    Mao M, Ryan D H and Altounian Z 1994 *Hyperfine Interact.* **92** 2163
[24] Stadnik Z M, Saida J and Inoue A 2001 *Ferroelectrics* **250** 297
    Stadnik Z M, Rapp Ö, Srinivas V, Saida J and Inoue A 2002 *J. Phys.: Condens. Matter* **14** 6883

[25] Stadnik Z M, Takeuchi T and Mizutani U 2000 *Mater. Sci. Eng.* A **294–296** 331
     Brand R A, Voss J and Calvayrac Y 2000 *Mater. Sci. Eng.* A **294–296** 666
     Stadnik Z M, Takeuchi T, Tanaka N and Mizutani U 2003 *J. Phys.: Condens. Matter* **15** 6365
[26] Jena P 1976 *Phys. Rev. Lett.* **36** 418
     Nishiyama K, Dimmling F, Kornrumph Th and Riegel D 1976 *Phys. Rev. Lett.* **37** 357
     Christiansen J, Heubes P, Keitel R, Klinger W, Loeffler W, Sandner W and Witthuhn W 1976 *Z. Phys.* B **24** 177
     Nishiyama K and Riegel D 1978 *Hyperfine Interact.* **4** 490
[27] Lin S, Li G and Zhang D 1996 *Phys. Rev. Lett.* **77** 1998
[28] Bianchi A D, Bommeli F, Felder E, Kenzelmann M, Chernikov M A, Degiorgi L, Ott H R and Edagawa K 1998
     *Phys. Rev.* B **58** 3046
[29] Edagawa K, Chernikov M A, Bianchi A D, Felder E, Gubler U and Ott H R 1996 *Phys. Rev. Lett.* **77** 1071